A Multiport Bidirectional LLC Resonant Converter for Grid-Tied Photovoltaic-Battery Hybrid System

Garry Jean-Pierre[1], Ahmad El Shafei[1], Necmi Altin[1,2], and Adel Nasiri[1]

[1]Center for Sustainable Electrical Energy Systems, University of Wisconsin Milwaukee, Milwaukee, USA
[2] Department of Electrical & Electronics Engineering, Faculty of Technology, Gazi University, Ankara, Turkey
jeanpie4@uwm.edu; aie@uwm.edu; altin@uwm.edu; nasiri@uwm.edu

***Abstract* — Bidirectional LLC resonant converters are becoming increasingly more attractive in grid-connected applications with integrated photovoltaic (PV) systems and energy storage systems (ESS). In this study, a multiport bidirectional LLC resonant converter for grid-tied systems is proposed. In addition, a region based control schema with a modified maximum power point tracking (MMPPT) control derived from the incremental conductance method is introduced to control both the forward (discharge mode) and backward (charge mode) operation of the proposed converter. The proposed topology consists of an integrated bidirectional converter for the battery system, a bidirectional LLC resonant converter, a voltage source inverter for grid-tied operation and the PV system. The proposed topology is modelled with MATLAB/Simulink and validated for different operation conditions.**

Keywords— Multiport converter, PV-battery hybrid system, Bidirectional LLC resonant converter,

I. INTRODUCTION

The requirement of building more compact systems that have the capability of integrating multiple energy sources and achieving both higher efficiency and power density has led to many outstanding innovations in power electronic converters. These include new concepts in power converter topologies and their control methods. Both unidirectional and bidirectional converters can be used for many applications, for instance small-scale photovoltaic (PV) systems and energy storage (ES), electric vehicle charging stations and other crucial systems that need uninterrupted power. However, in ES applications, bidirectional DC-DC converters (BDCs) play an important role in both charging and discharging the battery systems and managing energy flow between the sources when multiple sources are present. Therefore, BDCs are widely found in applications such as uninterruptible power supplies (UPS), PV systems and vehicle to grid (V2G) systems. These converters can be isolated, partially isolated or non-isolated based on power range and requirements of the application [1]-[4]. The bidirectional LLC topologies become an appealing choice for applications that require high frequency operation capability, high voltage level for renewable energy generation systems and high efficiency [4], [5].

Various topologies of bidirectional LLC resonant converters with an ES have been presented in literature. A bidirectional LLC resonant converter with symmetrical tanks was presented in [6]. The proposed topology doubles the equivalent switching frequency. This configuration aims to increase the converter power capability with reduced resonant components size while keeping equal operating frequency on both sides of the converter. In this configuration, the number of passive components is greatly increased. In [7], a secondary LLC resonant tank was introduced to achieve power transfer in both directions under wide voltage and load ranges. However, this configuration has a somewhat low efficiency and can be bulky due to the number of switches, the passive components and the three-winding transformer. A three-level LLC resonant converter with bidirectional power flow was introduced in [8]. The analysis of the gain values of this converter was carried out in order to obtain the power flow direction. Nonetheless, the use of extra flying capacitors and auxiliary clamping switches inflates the cost of the system and increases its complexity [9]. An LLC resonant converter with bidirectional power flow, containing automatic forward and backward transition mode was proposed in [10]. In this configuration, two active bridges are used with an added inductor. This model presents two modes of operations based on the gain. However, the voltage gain represents a limiting factor for the variation in switching frequency and how efficiently the system runs. To overcome the narrow voltage-gain problem of conventional LLC resonant converters, another topology suitable for wide voltage gain was introduced in [11]. This converter was designed to achieve high efficiency during wide voltage range operation. To realize soft switching, a bidirectional LLC resonant converter with different topology was introduced in [12]. This system works in two modes. In the forward mode, the system functions as a boost, while in the reverse mode, it works as a buck. According to [12], a major problem of this design is that at nonrated load conditions, there is an increase between the difference of the peak value of resonant voltage and the input voltage. This further affects the efficiency of the system. A topology for a secondary LLC resonant converter which utilized auxiliary switches and an inductor was presented in [13]. This converter was analyzed in both the forward and backward modes. In the forward mode, it works as a step up converter. In the reverse mode, the secondary side converter works as a half-bridge inverter.

Although these studies demonstrate topologies that improve upon previous research, all of them focus solely on two-port applications. In the case of hybrid systems, such as PV and

 978-1-7281-3587-8/19/$31.00 ©2019 IEEE

battery, the DC-DC converter has three-ports and, at minimum, the battery port has to be bidirectional. This converter can be designed by utilizing two LLC resonant converters or employing a three-winding transformer. In a limited number of studies, different LLC resonant converter topologies have been proposed to improve the power density and efficiency by removing the second converter and/or three-winding transformer [14], [15].

In this study, a multiport bidirectional LLC resonant converter for the grid-tied system is presented as an extension of [16] and a region based control scheme plus MMPPT control is introduced for a combination of battery and PV system. Different from past studies, this research utilizes three sources which are connected to the LLC resonant converter. The proposed integrated converter configuration and the control strategy eliminate two transformers or the three-port transformer requirement. As a result, the volume and efficiency of the converter and the transformer are greatly enhanced. The proposed design configuration and control methods were evaluated in MATLAB/Simulink.

II. Topology and Operating Principle of The Proposed System

A. Description

The topology of the proposed system is demonstrated in Fig. 1. The PV system is directly linked to the one port of the LLC converter and the battery is connected to the same port through a bidirectional buck-boost converter. The other port is connected to the grid via a three-phase voltage source inverter (VSI). Thus, multi-port partially isolated bidirectional DC-DC converter topology is obtained. When the PV system generates power, the Maximum Power Point Tracking (MPPT) is obtained via controlling the battery current. The grid connected VSI can export power supplied by PV and battery to the grid or it can charge the battery from the grid.

This converter is capable of operating in both forward and reverse modes. In both modes, four cases can be considered, as seen in Fig. 2. The power flow can be a combination of the PV source (PVS), the battery system (BS) and the grid source (GS). In forward mode, the power flow can be divided into three regions, as seen in Fig. 2 (a), (b) and (c). In Region-I, the power of the PVS is injected to the GS and the BS. In this region, the switch S_1 is kept off. Therefore, the battery is in charging mode and the S_{14} and S_{23} are also kept off, as seen in Fig. 3. In region-II, both the PVS and the BS supply power to the GS simultaneously. The switch S_2 is kept off, causing the battery to be in discharge mode. The switches S_{14} and S_{23} are also kept off,

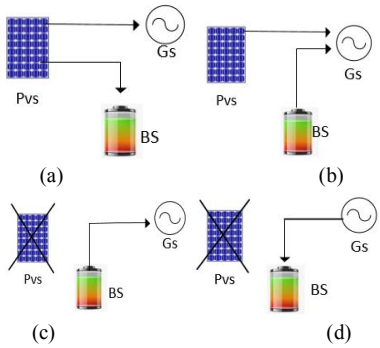

Fig. 2. Characterization of power distribution. (a) Forward mode Region-I (b) Forward mode Region-II (c) Forward mode Region-III (d) Reverse mode

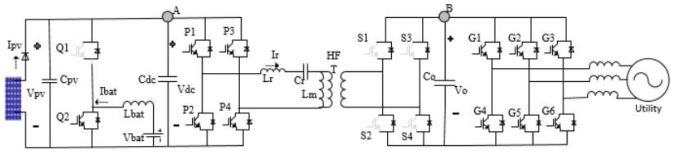

Fig. 3. Forward mode operation for region-I

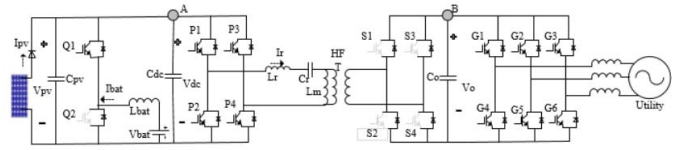

Fig. 4. Forward mode operation for region-II

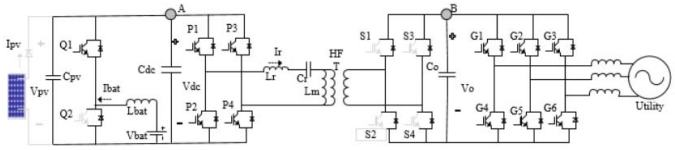

Fig. 5. Forward mode operation for region-III

as seen in Fig. 4. The PVS cannot supply the GS by itself. However, since it is assumed in this study that the amount of power exported to the grid is defined by a higher level controller, this operation condition represents a very special case, and thus it is not given in Fig. 2. In region-III, the PVS is not available. Therefore, the BS supplies power to the GS. In this region, the switch S_2 is kept off and the battery is in discharging mode and injecting power to the GS. The switches S_{14} and S_{23} are also kept off, as seen in Fig. 5. However, in reverse mode, the BS is always in charging mode. Thus, the GS is supplying power to the BS through the VSI and bidirectional buck-boost converter, as seen in Fig. 2 (d). In this mode, the switches P_{14}, P_{23} and S_1 are kept off while S_{14} and S_{23} are active, as demonstrated in Fig. 6.

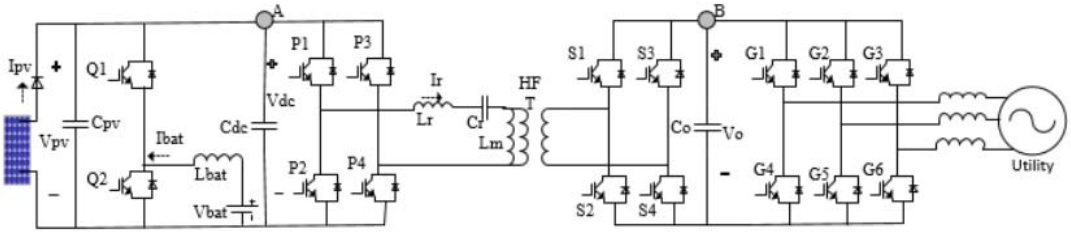

Fig. 1: The proposed converter configuration

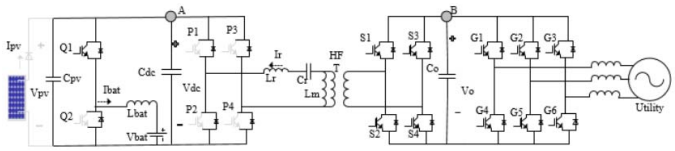

Fig. 6. Reverse mode operation

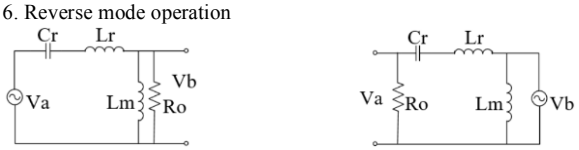

(a) (b)

Fig.7. Equivalent models of a bidirectional LLC resonant converter. (a) Forward mode. (b) Backward mode

B. *Analysis of Voltage Gain Characteristics of the Proposed LLC Resonant Converter*

As its name implies, an LLC resonant converter contains two inductors and one capacitor: the resonant inductor L_r, the magnetizing inductance of the transformer L_m, and the resonant capacitor C_r. Together, they form the resonant tank of the converter. Therefore, it has two resonant frequencies as given below. In the following equations, f_{r1} and f_{r2} stand for the first and second resonance frequency, respectively [17], [18], [23]:

$$f_{r1} = \frac{1}{2\pi\sqrt{L_r C_r}} \quad (1)$$

$$f_{r2} = \frac{1}{2\pi\sqrt{(L_r+L_m)C_r}} \quad (2)$$

Based on models in Fig. 7, the gain of the LLC resonant converter can be formulated as given below according to the Fundamental Harmonic Approximation (FHA) [13]-[22]:

$$K_{Forward} = \frac{aV_b}{V_a} = \frac{sL_m //R_o}{\frac{1}{sC_r}+ sL_r+ sL_m //R_o} \quad (3)$$

$$K_{backward} = \frac{aV_a}{V_b} = R_o + \frac{1}{sC_r} + sL_r + sL_m \quad (4)$$

To obtain simplified gain K equation, some parameters such as the quality factor Q, the ratio of the combined primary inductance to the resonant inductance m and the normalized frequency F_x, the reflected load resistance value R_{ac}, the transformer turn ratio a, and the switching frequency f_s are expressed:

$$Q = \frac{\sqrt{\frac{L_r}{C_r}}}{R_{ac}} \quad (5)$$

$$R_{ac} = \left(\frac{8}{\pi^2}\right)(a^2 \cdot R_o) \quad (6)$$

$$m = \frac{L_r + L_m}{L_r} \quad (7)$$

$$F_x = \frac{f_s}{f_{r1}} \quad (8)$$

Since the converter is not connected to a certain load resistance, the load resistance varies with the power level. The actual load resistance values for forward and backward operation modes can be calculated, as in (9) for the forward mode and (10) reverse mode, respectively:

$$R_o = \frac{V_o^2}{P_o} \quad (9)$$

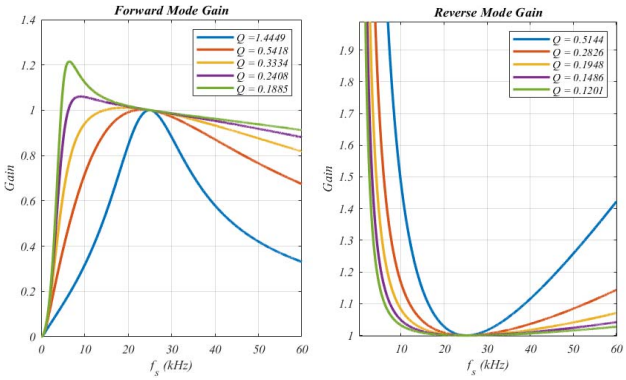

(a) (b)

Fig. 8. Gain trajectory of the proposed configuration for distinct Q values a) Forward mode b) Reverse Mode

$$R_o = \frac{V_{bus}^2}{P_{bat}} \quad (10)$$

As seen from Fig. 1, the proposed topology of the bidirectional LLC converter has a full bridge converter both at the input port (A) and at the output port (B). While the power is flowing from A to B in forward direction, it flows from B to A in backward mode. Thus, two gain values were obtained from the equations above and can be combined into equations (11) for the forward mode and (12) for the reverse mode.

$$K(Q, m, F_x) = \frac{1}{\sqrt{\left[1+\frac{1}{m}\left(1-\frac{1}{F_x^2}\right)\right]^2+\left(F_x-\frac{1}{F_x}\right)^2 \cdot Q^2}} \quad (11)$$

$$K(Q, m, F_x) = \sqrt{1+\left(F_x-\frac{1}{F_x}\right)^2 . Q^2} \quad (12)$$

As calculated from (11) and (12), the gains of the LLC resonant converter can be manipulated by regulating the switching frequency [13]. The gain trajectory of the proposed system for various resistance values are shown in Fig. 8 for both mode of operations. The parameter of the converter is specified based on the required gain values for the designated load range.

III. Proposed Control Strategy

The control approach was implemented to regulate the converter in both forward and reverse modes. The proposed control scheme is derived from Fig. 2 above. In Region-I and -II, during the forward mode of operation, the conventional Incremental Conductance (IC) method was modified to follow the Maximum Power Point (MPP) of the PV system through determining the current reference of the battery.

When the solar irradiation level is greater than the predefined lowest bound, the MMPPT technique is activated and adjusts the current reference for the battery. Thus the battery current (both charge and discharge current values) are determined based on the PV system operation condition. If the system is at the right hand side of the MPP, the battery current reference is reduced. Shrinking the battery current reference can be achieved by either reducing the power provided by the battery or increasing the power provided to the battery depending on the operation mode of the ESS. When the system is on left side of the MPP, the MMPPT augments the battery current reference, thus

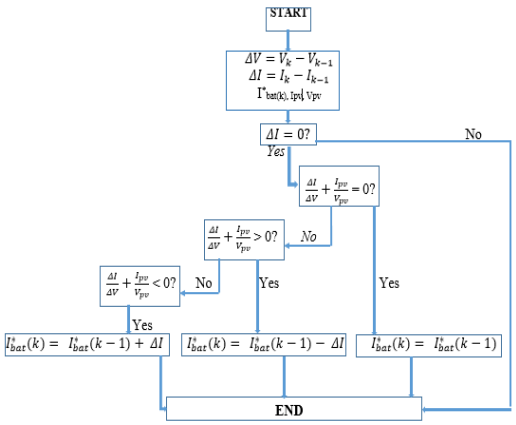

Fig. 9. Flowchart of the MMPPT controller

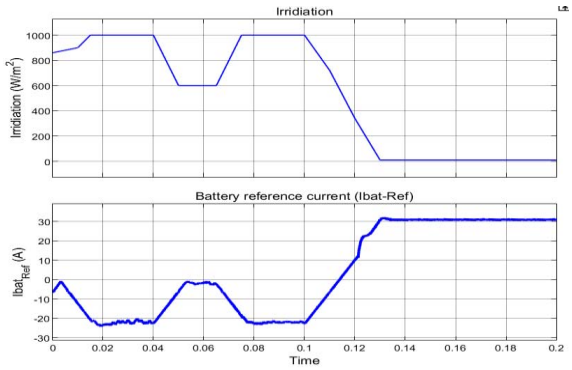

Fig. 10. MMPPT controller performance

boosting the charge capability or reducing the discharge capability. At the MPP, the MMPPT maintains the battery current reference constant. The flowchart defining the proposed MMPPT is given in Fig. 9, based on the conventional IC theory [24]. In Fig. 10, the solar irradiation value and corresponding battery reference current generated by the MMPPT algorithm is given. As seen, the MMPPT determines the battery current and state (charging or discharging) to keep the PV system operating point at its MPP.

In region-III of the forward mode, when PV power is not present or is too low, the mode detector algorithm, as seen in Fig. 12, disables the MPPT tracking and starts to operate in voltage control mode, as seen in Fig. 11(a). In this stage, a PI regulator is adopted to keep the DC bus voltage at the desired level. The PI regulator sets the battery current reference to maintain a constant voltage at the DC bus. In the reverse mode of operation, the battery current reference is identified by the mode detector algorithm which was generated by another PI controller that controls the battery voltage.

In reverse mode, the battery is charged by the grid and the VSI operates as a rectifier. This provides input voltage and energy for the LLC resonant converter. The bidirectional LLC resonant converter and bidirectional buck-boost converter charge the ESS by controlling battery voltage and current. The LLC resonant converter switching frequency is used to control V_o voltage in forward mode. Conversely, in reverse mode, it is controlled to maintain the DC bus voltage (V_{dc}) constant. Therefore, in the forward mode, P_1, P_2, P_3 and P_4 switches are controlled and secondary side switches are disabled. In the reverse mode, when the enable signal is activated, the switches S_1, S_2, S_3 and S_4 on the secondary side of the transformer are turned on and the switches P_1, P_2, P_3 and P_4 are turned off, as given in Fig. 11(b). In addition, the cascaded controller is used to control the LLC resonant converter in both operation modes. In the proposed control scheme, the current reference for the inner current loop is generated by the outer voltage control loop. The resonant current is filtered by a low pass filter whose cut-off frequency is designed to be equal to f_{r1}.

In this study, for the forward mode, it is assumed a higher level controller provides the active power reference for the VSI control system. The VSI is designed to operate at unity power factor, thus the reactive component is kept constant for both operation modes. In the reverse mode, the active component of the current is determined by a PI regulator that is designed to maintain the V_o at its desired level. The synchronous reference frame current control method, given in Fig. 11(c), is applied to control the three-phase currents injected into the grid.

IV. Simulation Results

In this paper, a multiport bidirectional LLC resonant topology and a control strategy comprising a MMPPT tracking strategy is presented for a grid-tied hybrid battery-PV system. MATLAB/Simulink simulation studies are performed to test the performance of the proposed configuration and control design. The over-all configuration utilizes a bidirectional LLC resonant converter, a bidirectional buck-boost converter and a grid-tied VSI. The system parameters are provided in Table 1.

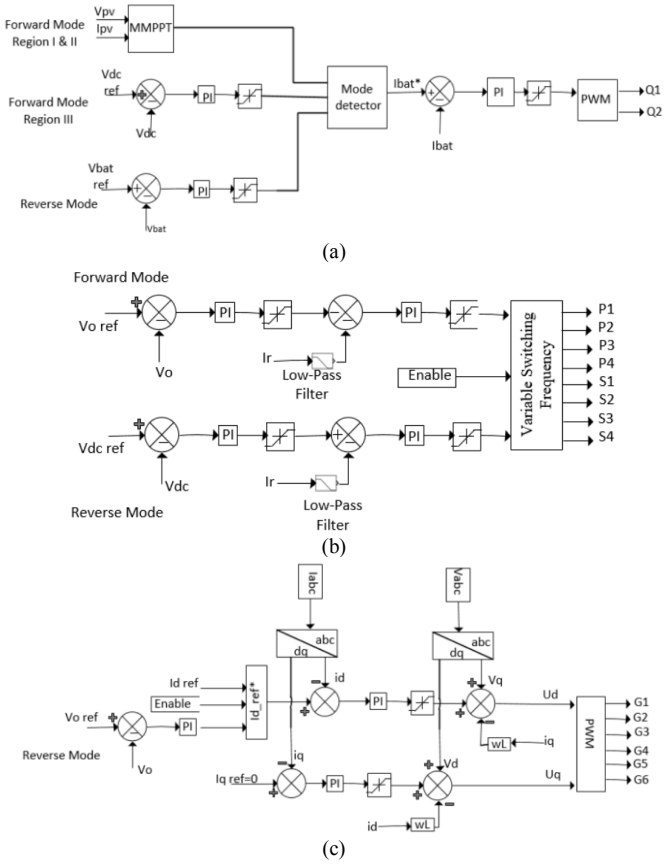

Fig. 11. Control of the proposed topology a) The output voltage control b) The MMPPT and battery charge/discharge controller (c) The VSI control

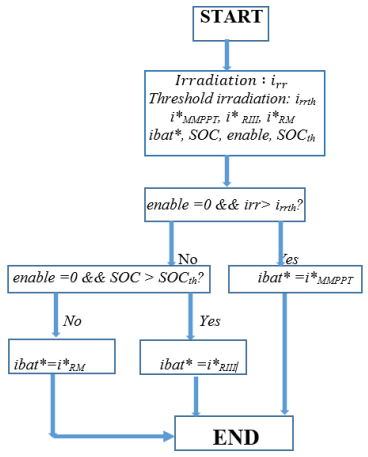

Fig. 12. Mode detector algorithm

In forward mode, the current component for active power of the VSI system is kept constant at 20A and reactive power is kept constant at 0A. In Region-I, the PV power is higher than the power injected into the grid. The remaining power is stored in the battery system. In region-II, the PV power is less than the required grid power. The battery compensates for the lacking power. In region-III, the PV power is not present and the battery delivers all the power to the grid. In reverse mode, energy is exported from the grid to the battery system. The voltage and current waveforms of the battery system, the PV system and the grid for all operation modes are given in Fig. 13. In Fig. 13, the grid power is represented by its mean value, and the grid current by its root-mean-square value. Therefore, their variations have some slope. As seen from the figure, after a small oscillation around the MPP, the MMPPT determines the battery current reference for the current controller of the bidirectional buck-boost converter. Thus, by controlling the battery current, the PV system is forced to operate at its MPP. At the same time, the bidirectional LLC resonant converter keeps the output voltage at the desired value and provides DC energy for the VSI. Then the VSI exports the energy to the three-phase AC grid.

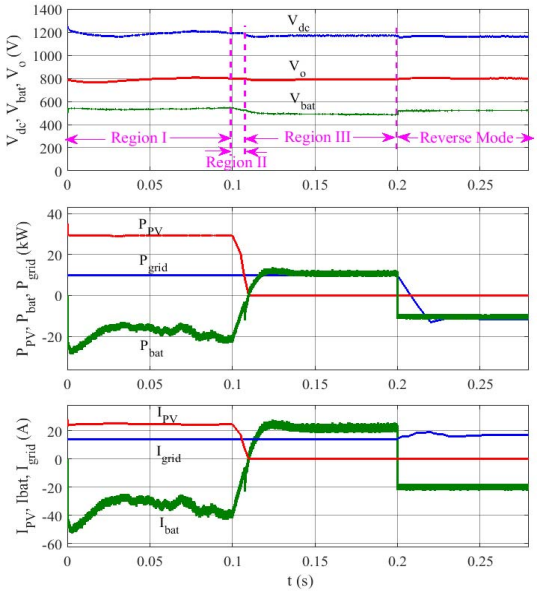

Fig. 13. Operation waveforms of the proposed system for all three regions and reverse mode.

TABLE I. SYSTEM PARAMETERS

Parameters	Value
Resonant inductor, L_r	10µH
Magnetizing inductor, L_m	250µH
Resonant capacitor, C_r	4µF
Switching frequency (LLC resonant converter)	20-60kHz
Switching frequency (Buck-Boost Converter)	30 kHz
Switching frequency (VSI)	10 kHz
Output voltage, V_o	800V
Battery voltage, V_{bat}	460-540V
Grid voltage (phase to neutral, rms) and frequency, V_g,f_g	230V.50Hz
Inductance (Buck-Boost Converter), L_{bat}	0.7mH
VSI output filter, L_{inv}	2 mH

At t=0.1s, when the irradiation and the PV power start to decrease, the MMPPT regulates the battery current reference to maintain the PV system at MPP. When PV power is less than the predefined bound, the MMPPT is deactivated and the battery current is regulated to keep the V_{dc} constant. In this region (region-III), the battery system provides all the required energy. The LLC resonant converter is still controlled to keep the output voltage (V_o) constant. In Regions-I, -II, and -III, the battery current is the main variable that controls the system. When the system operates in reverse mode, the battery is charged from the grid. As seen in Fig. 13, the proposed system can work in all the regions and provides a smooth transition among the operation modes.

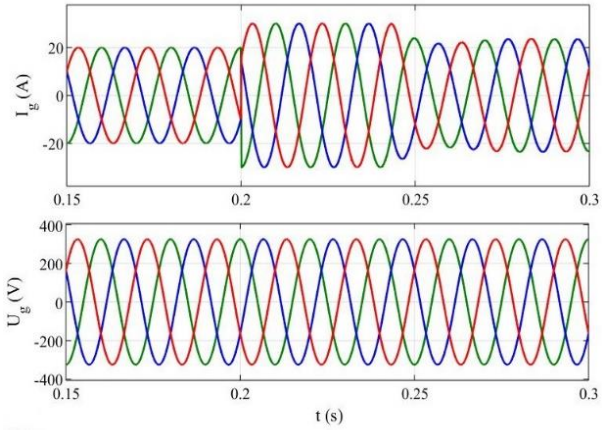

Fig. 14. Three-phase grid currents and voltages.

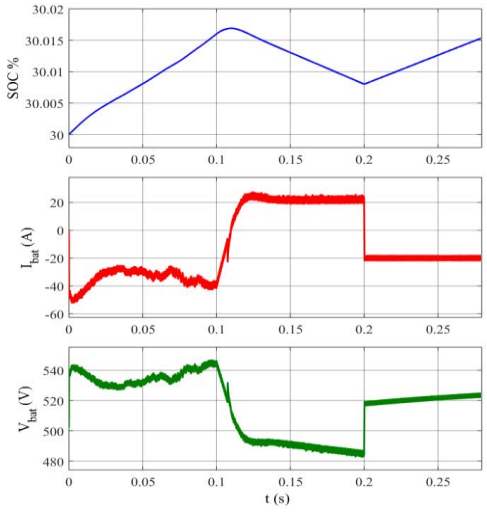

Fig. 15. The battery voltage, current and state of charge values.

In Fig. 14, three-phase currents injected to the grid and three-phase grid voltages are seen. Until t=0.2s, the inverter exports power supplied by the PV and/or battery system to the grid. For this operation mode, it is assumed that a higher level controller provides current reference (20A) to the inverter. At t=0.2s, the inverter operation mode switches and the battery system is charged from the grid. In this operation mode, the reference value for the current drawn from the grid is determined by the PI controller, which was designed to keep the DC bus voltage of the inverter (also V_o) at the desired value (800V). Therefore, the grid current values vary after this moment. In practical application, the maximum current should be limited to protect the hardware. In this study, its peak value is limited at 30A. Similarly, the battery charge current is limited at 20A for this operation mode. As seen in Fig. 13, the proposed inverter has fast transient response and excellent steady state performance in both modes. Three-phase currents are all in sinusoidal waveforms, and the total harmonic distortion (THD) value is 1.35% and 1.27% for inverter and rectifier modes of operation, respectively. The ESS voltage, current and state of the charge (SOC%) are shown in Fig. 15. The initial SOC value is 30%. The battery is in charging mode in Region-I and reverse mode. It is in discharging mode in Regions-II and -III. The operation modes can also be tracked from battery voltage.

V. Conclusion

In this paper, a multiport bidirectional LLC resonant converter is provided for grid-tied PV-battery hybrid systems. While the PV component is directly linked to the LLC resonant converter port, the battery is configured through the bidirectional buck-boost converter. In addition, the three-phase VSI inverter is used to import and export the energy to and from the three-phase AC grid. A control strategy is introduced to regulate the voltage, current and power between the ports for all operation modes. It is shown that the proposed configuration operates in both operation modes, including all three regions, successfully. Additionally, the power flow between the ports are stable and precise, and main voltage values at every port are maintained constant for any operation mode.

Acknowledgment

Dr. Necmi Altin thanks financial support from the Scientific and Technological Research Council of Turkey (TUBİTAK) BIDEB-2219 Postdoctoral Research Program.

References

[1] M. Uno, R. Oyama, and K. Sugiyama, “Partially isolated single-magnetic multiport converter based on integration of series-resonant converter and bidirectional PWM converter,” IEEE Trans. Power Electron., vol. 33, no. 11, pp. 9575–9587, 2018.

[2] L. Chen, H. Wu, P. Xu, H. Hu, and C. Wan, “A high step-down non-isolated bus converter with partial power conversion based on synchronous LLC resonant converter,” 2015 IEEE Appl. Power Electron. Conf. and Exposition (APEC), 2015.

[3] D. Huang, X. Wu, and F. C. Lee, “Novel non-isolated LLC resonant converters,” 2012 Twenty-Seventh Annual IEEE Appl. Power Electron. Conf. and Exposition (APEC), 2012.

[4] T. Labella, W. Yu, J.-S. Lai, M. Senesky, and D. Anderson, “A bidirectional-switch-based wide-input range high-efficiency isolated resonant converter for photovoltaic applications,” IEEE Trans. Power Electron., vol. 29, no. 7, pp. 3473–3484, 2014.

[5] M.-H. Ryu, H.-S. Kim, J.-H. Kim, J.-W. Baek, and J.-H. Jung, “Test bed implementation of 380V DC distribution system using isolated bidirectional power converters,” 2013 IEEE Energy Conversion Congr. and Exposition, 2013.

[6] S. Zong, X. He, H. Luo, W. Li, and Y. Deng, “High-power bidirectional resonant DC–DC converter with equivalent switching frequency doubler”, IET Renew. Power Gen., vol. 10, no. 6, pp. 834–842, Jan. 2016.

[7] E.-S. Kim, J.-H. Park, J.-S. Joo, S.-M. Lee, K. Kim, and Y.-S. Kong, “Bidirectional DC-DC converter using secondary LLC resonant tank”, 2015 IEEE Appl. Power Electron. Conf. and Exposition (APEC), 2015.

[8] T. Jiang, J. Zhang, Y. Wang, Z. Qian, and K. Sheng, “A bidirectional three-level LLC resonant converter with PWAM control”, 2013 1st International Future Energy Electronics Conference (IFEEC), 2013.

[9] S. M. S. I. Shakib, S. Mekhilef, and M. Nakaoka, “Dual bridge LLC resonant converter with frequency adaptive phase-shift modulation control for wide voltage gain range”, 2017 IEEE Energy Conversion Congr. and Exposition (ECCE), 2017.

[10] T. Jiang, J. Zhang, X. Wu, K. Sheng, and Y. Wang, “A bidirectional LLC resonant converter with automatic forward and backward mode transition”, IEEE Trans. Power Electron., vol. 30, no. 2, 757–770, 2015.

[11] Y. Shen, H. Wang, F. Blaabjerg, A. A. Durra, and X. Sun, “A fixed-frequency bidirectional resonant DC-DC converter suitable for wide voltage range”, 2017 IEEE Appl. Power Electron. Conf. and Exposition (APEC), 2017.

[12] C. Zhang, Z. Gao, and X. Liao, “Bidirectional DC–DC converter with series-connected resonant tanks to realize soft switching”, IET Power Electronics, vol. 11, no. 12, pp. 2029–2043, 2018.

[13] E.-S. Kim, J.-H. Park, Y.-S. Jeon, Y.-S. Kong, S.-M. Lee, and K. Kim, “Bidirectional secondary LLC resonant converter using auxiliary switches and inductor”, IEEE Appl. Power Electron. Conf. and Exposition, 2014.

[14] B. Mangu, S. Akshatha, D. Suryanarayana, and B. G. Fernandes, “Grid-connected PV-Wind-battery-based multi-input transformer-coupled bidirectional DC-DC converter for household applications,” IEEE Trans. Emerg. Sel. Topics Power Electron., vol. 4, no. 3, pp. 1086–1095, 2016.

[15] J. Zeng, W. Qiao, and L. Qu, “An isolated three-port bidirectional DC-DC converter for photovoltaic systems with energy storage,” 2013 IEEE Industry Applications Society Annual Meeting, 2013.

[16] G. Jean-Pierre, N. Altin, and A. Nasiri, “A Three-Port LLC Resonant Converter for Photovoltaic-Battery Hybrid System,” 2019 IEEE Transportation Electrification Conference (ITEC), 2019.

[17] Y. Wei, N. Altin, Q. Luo, and A. Nasiri, “A high efficiency, decoupled on-board battery charger with magnetic control,” 2018 7th International Conf. on Renewable Energy Research and Applications (ICRERA), 2018.

[18] Y. Wei, Q. Luo, X. Du, N. Altin, A. Nasiri and J. M. Alonso, "A Dual Half-bridge LLC Resonant Converter with Magnetic Control for Battery Charger Application," IEEE Trans. Power Electron. doi: 10.1109/TPEL.2019.2922991

[19] M. Arazi, A. Payman, M. B. Camara and B. Dakyo, "Control of isolated DC/DC resonant converters for energy sharing between battery and supercapacitors," 2018 7th International Conference on Renewable Energy Research and Appl. (ICRERA), Paris, 2018, pp. 1049-1054.

[20] J. Liu, J. Zhang, T. Q. Zheng, and J. Yang, “A modified gain model and the corresponding design method for an LLC resonant converter,” IEEE Trans. Power Electron., vol. 32, no. 9, pp. 6716–6727, Sep. 2017.

[21] Zhang, Jiepin, et al. “An LLC-LC Type Bidirectional Control Strategy for an LLC Resonant Converter in Power Electronic Traction Transformer”, IEEE Trans. Ind. Electron., vol. 65, no. 11, 2018, pp. 8595–8604.

[22] Yang, S., Shoyama, M., Zaitsu, T., Yamamoto, J., Abe, S., et al. 2012. Detail operating characteristics of Bi-directional LLC resonant converter. 2012 International Conference on Renewable Energy Research and Applications (ICRERA).

[23] Hiroyuki Haga, Hidenori Maruta, Fujio Kurokawa, “Analysis of Voltage Gain Tolerance due to the Resonant Circuit Variation of LLC Resonant Converter” 2016 International Conference on Renewable Energy Research and Applications (ICRERA).

[24] N. Altin and E. Ozturk, “Maximum power point tracking quadratic boost converter for photovoltaic systems,” 2016 8th International Conference on Electronics, Computers and Artificial Intelligence (ECAI), 2016.